Design of Box Girders of Deformable Cross Section

RICHARD N. WRIGHT, Department of Civil Engineering,
University of Illinois, Urbana

A procedure is presented for design of the spacing and proportions of diaphragms in box-girder bridges. The objective is to hold transverse flexural distortion stresses and warping stresses, arising from deformation of the cross section, to limits that ensure safe performance and an economical design. Complex, refined analytic methods are available for analysis of a box-girder structure of defined proportions loaded in a particular manner. The procedure supplements these methods by providing a clear view of interactions among proportions, loadings, and response, and helps the designer work efficiently toward a satisfactory design.

•THE BOX-GIRDER FORM offers considerable advantage for highway bridges because its high torsional stiffness leads to nearly uniform transverse distribution of flange stresses for a transversely nonuniform distribution of load. Although the conventional theory of torsion assumes that a cross section remains undeformed, a load, often called a torsional load, can tend to deform a cross section as well as twist it (Fig. 1). For usual bridge-girder proportions, longitudinal warping stresses arising from deformation of the cross section are far greater than, and add to, the longitudinal stresses arising from restraint of warping in torsion. The transverse flexural stresses arising from deformation of the cross section are completely ignored in elementary torsion analysis, which assumes a rigid cross section. However, these stresses are quite important in bridge design. They undergo full reversal as lanes on alternate sides of the bridge are loaded and, if excessive in magnitude, could lead to fatigue failure at the junction of web and flange plates.

Deformation of the cross section of a box girder can economically be restricted to a tolerable amount by appropriate sizing and spacing of interior cross bracing or diaphragms. The principal objective of this paper is to present a simple and direct procedure for accomplishing this phase of design. The procedure is approximate, but it accounts rationally for the principal parameters governing the response of box girders to loadings that tend to deform their cross sections. Complex, refined analytic methods are available (1, 2, 3, 4) for analysis of a structure of defined proportions loaded in a particular manner. The procedure presented here supplements these methods by providing a clear view of interactions between proportions, loadings, and response, and helps the designer work efficiently toward a satisfactory design.

APPROXIMATE ANALYSIS OF MULTICELL GIRDERS

The analysis presented here is based on the BEF (beam on elastic foundation) analogy (5) for analysis of the effects of deformation of the cross section of single-cell box girders. The BEF analogy can be exact for negligible shear deformation in the single-cell box, but, for simplicity, an approximation of the warping stiffness of the box cell is used in the expressions given in the Appendix. A further approximation is

Paper sponsored by Committee on Steel Superstructures and presented at the 48th Annual Meeting.

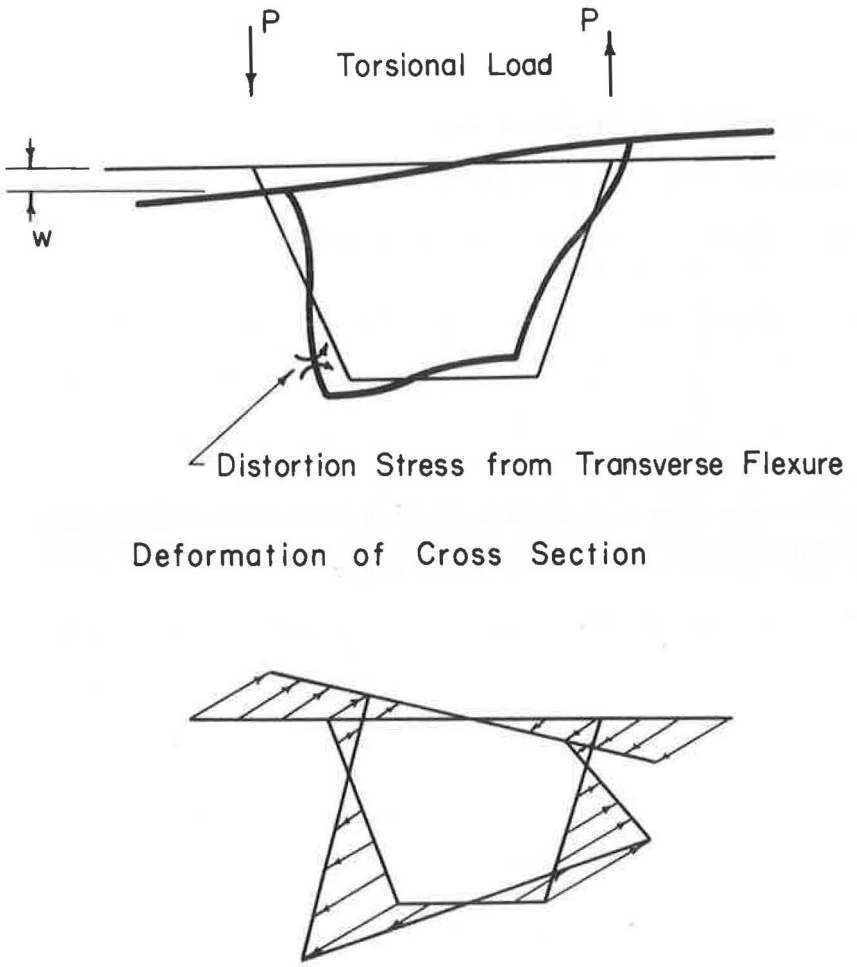

Figure 1. Response of box girder of deformable cross section to torsional load.

added in the application to multicell box girders. The complex interaction of deformation of the cross section and torsion in multicell girders is neglected; an estimate is made of the portion of the loading that tends to deform the most severely loaded cell, and this cell is assumed to respond independently of the remainder of the cross section.

The dead load of a straight box-girder bridge is quite uniformly distributed in the transverse direction and does not deform the cross section appreciably. The live loading is of direct interest because it can produce substantial deformation of the cross section. The effect of wheel loads at a particular cross section is obtained by first computing the "holding forces" required to prevent vertical deflections at the deck-web intersection. The procedure is illustrated in Figure 2. It is assumed that the deck acts as a beam strip running transversely, and only vertical holding forces are evaluated because the rotational stiffness of the webs is small compared to that of the deck. The equilibrants of the holding forces then are applied as a loading on the box girder,

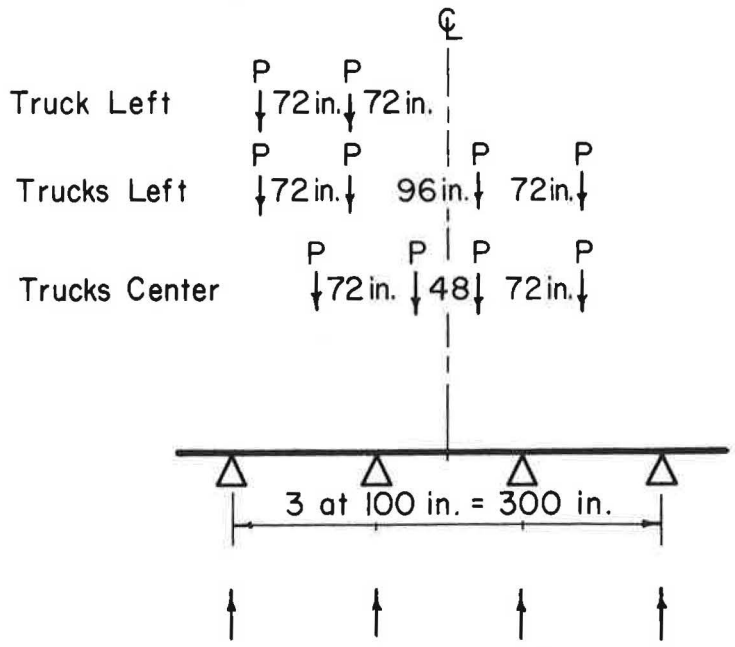

Truck Left	1.06P	1.07P	-.14P	.01P
Trucks Left	1.05P	1.18P	1.46P	.31P
Trucks Center	.27P	1.73P	1.73P	.27P

Figure 2. Loading on box girder caused by wheel loads on deck.

and its response is evaluated. Forces in the webs and bottom flanges arise only from this loading because these elements are unstressed while the holding forces act.

The loading generally includes a flexural component that produces simple bending of the cross section. This component is removed from the total load to arrive at the torsional component that tends to deform the cross section. The procedure is shown in Figure 3. Line 1 shows the total load at the cross section, which is obtained in the manner shown in Figure 2. Line 2 shows the flexural component, assuming, for simplicity, that there is a negligible contribution of the webs to the flexural stiffness. Line 3 shows the net torsional component. Line 4 illustrates the principal assumption in this development. The direct torsional load acting on each cell is obtained by beginning at one side of the cross section and indicating the torsional load on each cell for no change in the total force at any flange-web intersection. The most severely loaded cell, the middle one in this case, is considered in the analysis by the BEF analogy.

A similar approach is used to define the most severely loaded cell for separated-cell box girders. One additional step is needed as shown in Figure 4. If direct torsional load occurs where there is no cell, it is assigned to adjacent cells as shown in line 5.

The most complete results of the refined method of analysis for evaluation of the accuracy of this approach are those of Abdel-Samad (6). The work includes analyses of a three-cell box girder of reinforced concrete proportions for different spacings of deformable interior diaphragms. The box-girder properties are as follows: span = 100 ft with simple end supports; depth = 96 in.; width of each cell = 120 in.; thickness

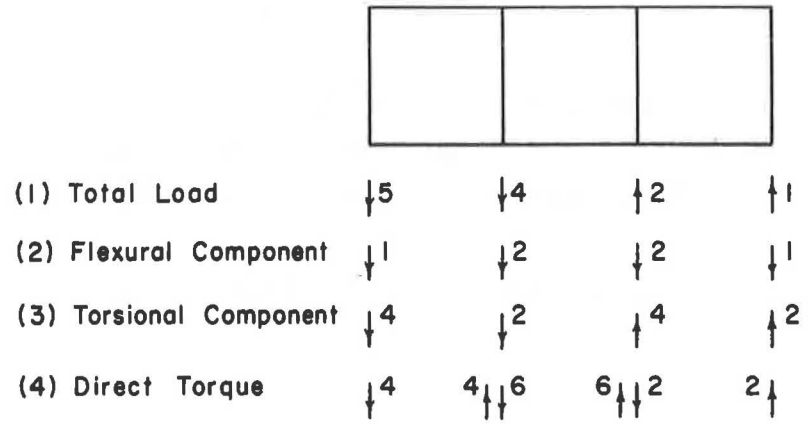

Figure 3. Cell loading for multicell girders with contiguous cells.

of all plates and interior diaphragms = 6 in.; E = 3,000 ksi (thousand pounds per square inch); and Poisson's ratio = 0.1. A number of different arrangements of loading at midspan are shown in Figure 5. By the procedure of Figure 3, each arrangement corresponds to a torsional load of 10 kips on the most severely loaded cell. Table 1 gives the results of analysis by the BEF analogy for this loading and the results obtained by Abdel-Samad by the refined method for the actual load configurations on the three-cell girder. Details of BEF analogy computations are given later in the design example.

Column 1 of Table 1 gives results for only end diaphragms present. The warping stress is denoted as σ_w and the transverse flexural stress is denoted as σ_t. The BEF analogy represents the results of load 1 quite well (for this loading each cell is subjected to essentially equal torsional load), but it is quite conservative for loads 2, 3, and 4 (for these loads the less severely loaded cells appear to relieve the one most severely loaded). Columns 2 and 3 consider the loading at midspan to be halfway between diaphragms spaced at 267 and 133 in. respectively. Note that response to the different loadings becomes more nearly the same as interior diaphragms are introduced and their spacing is reduced. Note also that the BEF analogy predicts the behavior quite accurately with the interior diaphragms present. Column 4 gives the behavior

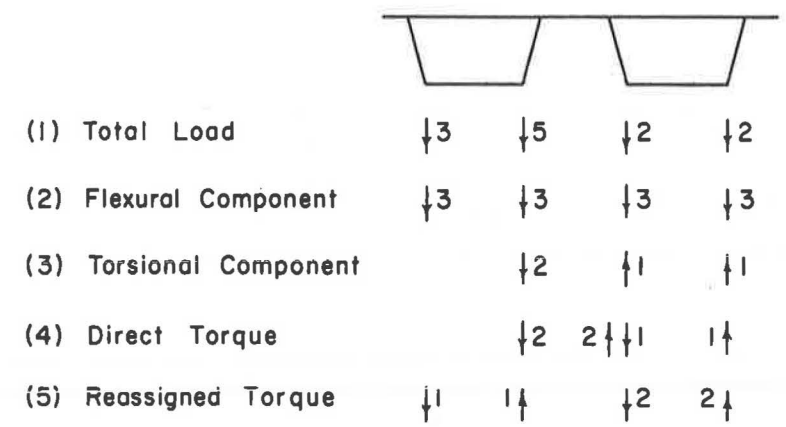

Figure 4. Cell loading for multicell girders with separated cells.

for a single interior diaphragm at the location of the load. The BEF analogy gives an accurate representation of the transverse flexural stress but underestimates the warping stress because most of the warping stress results from restraint of warping in torsion rather than from deformation of the cross section. The magnitude of this warping stress for a rigid cross section is given in column 5.

The accuracy of the BEF analogy in predicting the behavior of multicell, separated-cell, steel box girders is shown by data given in Table 2. The box girders are of the form of two trapezoidal cells with a composite reinforced concrete deck. Proportions of the girders are almost identical with the girder that is discussed later in the design example: E = 30,000 ksi for steel and 4,130 ksi for concrete; Poisson's ratio = 0.3 for steel and 0.15 for concrete; deck thickness = 7 in.; web thickness = $^3/_8$ in.; bottom flange = 80 in. wide by $^9/_{16}$ in. thick; total deck width = 400 in.; depth from center of deck to center of bottom flange = 65 in.; and a simple span = 100 ft, with no interior diaphragms and rigid diaphragms at the ends. The shape of the cross section and the load configurations at midspan are shown in Figure 6; by the procedure illustrated in Figure 4, each loading is equivalent to a 10-kip torsional load on the most severely loaded cell. Three girders are considered that differ only in the detail of transverse stiffeners: girder A has none, girder B has 6- by $^3/_8$-in. plate stiffeners at 52-in. spacing on the web plates, and girder C has 6- by $^3/_8$-in. stiffeners at 52-in. spacing on both web and bottom flange plates.

Results of the refined method given in Table 2 are obtained by the plate element

TABLE 1

COMPARISON OF BEF ANALOGY WITH REFINED METHOD FOR THREE-CELL BOX GIRDER WITH INTERIOR DIAPHRAGMS

Method of Analysis	Spacing of Diaphragms (in.)				
	1,200 (1)	267 (2)	133 (3)	600 (4)	Rigid Section (5)
BEF analogy					
σ_w, ksi	0.030	0.022	0.012	0.001	0
σ_t, ksi	0.055	0.007	0.002	0.002	0
Refined method[a]					
Load 1					
σ_w, ksi	0.030	0.016	0.010	0.004	0.003
σ_t, ksi	0.058	0.004	0.002	0.002	0
Load 2					
σ_w, ksi	0.020	0.013	0.009	0.002	0.001
σ_t, ksi	0.026	0.004	0.002	0.002	0
Load 3					
σ_w, ksi	0.010	0.008	0.005	0.001	0.000
σ_t, ksi	0.027	0.003	0.002	0.001	0
Load 4					
σ_w, ksi	0.015	0.012	0.008	0.002	0
σ_t, ksi	0.021	0.005	0.003	0.002	0

[a]Load configurations and positions of maximum stresses are shown in Figure 5.

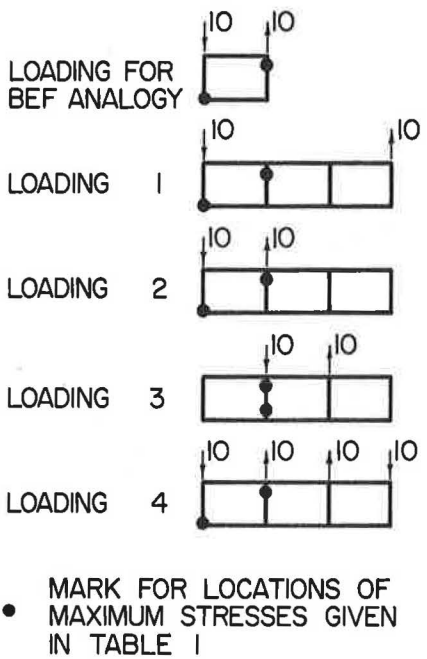

Figure 5. Arrangements of torsional load on three-cell box girder.

TABLE 2

COMPARISON OF BEF ANALOGY WITH REFINED METHOD FOR TWO-CELL COMPOSITE BOX GIRDERS

Method of Analysis	Structure					
	Girder A		Girder B		Girder C	
	σ_w ksi	σ_t ksi	σ_w ksi	σ_t ksi	σ_w ksi	σ_t ksi
BEF analogy	2.1	3.1	0.67	4.6	0.51	3.3
Refined method[a]						
Load 1	1.12	0.58	0.60	3.50	0.45	2.74
Load 2	0.98	0.77	0.54	3.66	0.40	2.84
Load 3	0.84	0.66	0.43	2.98	0.33	2.44
Load 4	0.84	0.76	0.49	3.86	0.35	2.94

[a]Load configurations and positions of maximum stresses are shown in Figure 6.

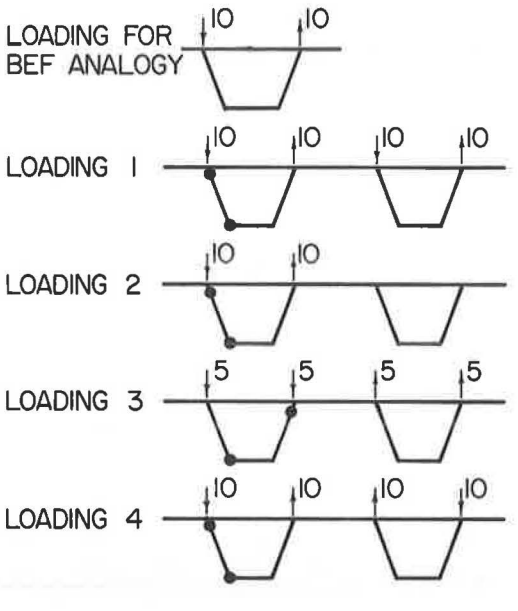

Figure 6. Arrangements of torsional load on steel box girder.

method (1) for a nine-Fourier-term expansion of the loading. The transverse flexural stresses, σ_t, are essentially converged, but peak magnitudes of the warping stresses, σ_w, may be as much as 20 percent greater than the given values.

The various loading arrangements are indeed quite equivalent in terms of peak warping and distortion stresses, much more so than those for the contiguous cell girder with no interior diaphragms (Table 1). The transverse stiffeners have appreciable effect on warping and distortion stresses. The addition of transverse stiffeners on the web, girder B, improves the load distribution by nearly a factor of 2 as evidenced by the reduction in peak warping stress from that of girder A. However, the peak distortion stresses are much higher for girder B because the curvature of deformation of the cross section acts through the stiffener height of 6 in. rather than through the plate half thickness of $^3/_{16}$ in. Addition of transverse stiffeners to the bottom flange, girder C, reduces both the peak warping and distortion stresses. However, this is an expensive way to improve the behavior of the box girder. Addition of interior diaphragms is a much more economical means of obtaining the objective.

The BEF analogy gives results that compare quite well with the refined-method results for girders B and C. Data in Table 1 suggest that the agreement could be expected to improve if interior diaphragms were considered. The BEF analogy is very conservative for unstiffened girder A. However, this girder is so deformable in cross section that it does not behave at all like a box girder of rigid cross section. The peak warping stress of about 1 ksi is equivalent to the stress that would be produced by a flexural loading of 6 kips at each of the four intersections of deck and web. Good lateral distribution of markedly eccentric loads is not achieved.

The comparisons of the BEF analogy with refined methods of analysis given in Tables 1 and 2 show that the BEF analogy may give very conservative results when applied to a box girder with very widely spaced diaphragms or a very deformable cross section. However, the BEF analogy correctly reflects the influence of altered diaphragm spacing (Table 1) or stiffening of the elements of the cross section (Table 2), and gives reasonably accurate results when structural proportions are such that behavior approximates that of a box girder of rigid cross section. The approximate extension of the BEF analogy to multicell girders is considered to be accurate enough for use in design. The effects of parameter variations on peak warping and distortion stresses are correctly reflected (the warping and distortion stresses being secondary stresses that the designer wishes to keep small rather than to hold close to a relatively large allowable level while proportions are varied for economy).

OUTLINE OF DESIGN PROCEDURE

The need to account for deformation of the cross section in the design of box-girder bridges is illustrated in Figure 7, which shows maximum stresses for a highway live loading. The proportions of the two-cell, steel box girder with composite concrete deck are the same as those of the 100-ft span bridge given earlier except that proportions for the midspan region apply throughout the length and no interior diaphragms

are present. The loads are AASHO HS20-44 trucks on one or two lanes, and analysis is by the plate element method (1).

Peak live-load flange stress occurs when both lanes are loaded and each truck moves toward the center of the bridge. The deformation of the cross section for this load arrangement produces warping stresses that lead to a peak flange stress almost 15 percent greater than the average flange stress at the section of maximum moment. This is a considerably better load distribution than that which would occur in a comparable bridge with 4 I-girders. The behavior of the bridge is perhaps more critical when one lane is loaded by a truck at the outside of its lane. Although this loading produces maximum warping stresses with a large torsional component, it does not control design of the flanges because the flexural component of loading is halved. However, it produces a peak distortion stress of -11.9 ksi in the web stiffener at its connection to the top flange; when a truck is in the outside of the other lane, the stress at this point would reverse to +11.0 ksi. The potential number of cycles of such load reversal is high, and the peak stress occurs at a fillet-welded splice. Thus, a fatigue problem is strongly suggested.

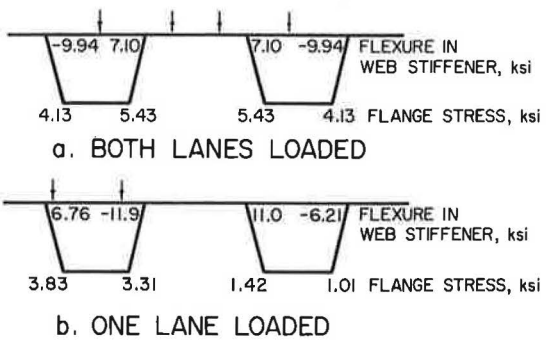

Figure 7. Stresses from highway loadings in steel box girder without interior diaphragms.

It is recommended that the box girder be stiffened by interior cross bracing or diaphragms of such spacing and stiffness that the peak distortion stresses are kept small enough to preclude fatigue damage. This approach has two concomitant advantages: (a) the peak warping stresses will be reduced simultaneously, leading to better load distribution and more economical flange proportions; and (b) the interior diaphragms may be shop-fabricated with the steel section to make it easier to handle before the deck slab is poured in the field.

Basic proportions of the cross section are established by conventional means considering only the flexural component of the loading and assuming that the potentially excellent load-distributing characteristics of the box-girder form will be attained. The BEF analogy is then used to space and proportion interior diaphragms so that high distortion stresses are avoided and good load distribution is realized. The steps of the design process are as follows:

1. The deck is designed to support vehicle wheel loads. It may be treated as a continuous plate simply supported by undeflecting line supports at the girder webs. The procedures given by AASHO (7) for reinforced concrete decks and AISC (8) for steel plate decks appear applicable to closed-section girder bridges. Only rarely will the deck design require revision because of longitudinal stresses caused by overall bridge response or additional transverse flexural stresses induced as the bridge deflects.
2. The bridge cross section is designed as if it were a beam in flexure without twist. Dead load, live load, and impact are considered and flange stresses are assumed to be uniform. At this stage, the live plus impact moment is increased about 10 percent to account for warping stresses. Conventional beam theory may be used to account for continuity and changes in the moment of inertia along the span.
3. Web stiffeners are proportioned for the shear. Shear distribution procedures giving satisfactory results for open-section bridges should be suitable for obtaining design shears. The high torsional stiffness of box girders does not substantially improve distribution of shear stresses because the controlling shear at any section occurs for loads adjacent to the section. Shears corresponding to the reactions on the deck acting as a beam strip on undeflecting supports, as in Figure 2, would be conservative.
4. BEF analogy parameters are computed for different cross sections of the bridge. The maximum twist exerted by the live loading on any one cell of the cross section is evaluated by procedures described in the previous section.

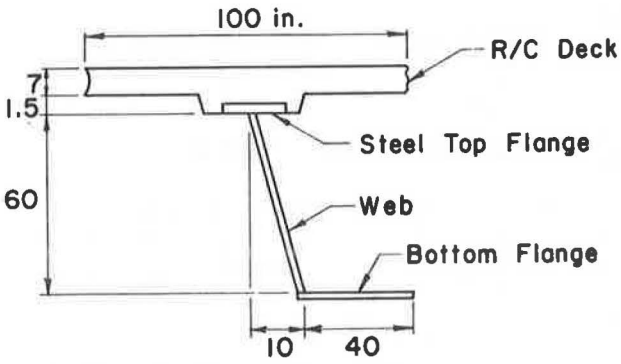

Figure 8. Element of box girder cross section.

5. Diaphragm spacing and stiffness requirements for control of distortion stress are evaluated. Usually, it is possible to choose an economical, convenient spacing of diaphragms and then to select the stiffness required to control distortion stresses.

6. Diaphragms or cross bracing, proportioned for stiffness, are checked for stresses.

7. Warping stresses are evaluated for the established cross section and diaphragm proportions. Appropriate sums of live plus impact stresses from uniform flexure and warping are compared with allowable values.

8. If the section is overstressed, it normally will be economical to revise flange proportions or diaphragm spacing rather than to revise diaphragm proportions. Warping stresses are not markedly changed by small changes in diaphragm stiffness, as is shown later in Figure 11. It is necessary to repeat steps 4 to 7 only for substantial changes in the proportions of the cross section.

At first glance, steps 4 to 7 of the design process may appear complex. However, the procedure gives a rational treatment of warping stresses and diaphragm proportioning that appears more reliable than conventional load distribution, diaphragm spacing, and sizing criteria for open-section girder bridges. Furthermore, these processes are outlined in some detail and actually involve fewer computations and iterations than the familiar processes of steps 1 and 2.

DESIGN EXAMPLE

The suggested design procedure is illustrated for a two-lane bridge of a 100-ft span with a composite reinforced concrete deck supported by two trapezoidal steel box girders. Standard AASHO HS20-44 loading (7) is used.

AASHO design criteria and the design procedures described in a recent U.S. Steel Corporation manual (9) are used where applicable. A-36 steel is used for the girder elements. Steps 1 and 2 of the design process outlined earlier are carried out by conventional procedures and are not discussed in the example.

A single-web element constituting one-fourth of the whole cross section is shown in Figure 8. The material properties used in design are as follows: for the deck, f'_c = 4,000 psi and n = 8; for the steel elements, F_y = 36 ksi, ν = 0.30, and E = 29,000 ksi.

The element of the cross section is proportioned at midspan and quarter points for a live loading consisting of one-fourth the moment of two lanes of HS20-44 truck loading plus a 10 percent allowance for warping stress. Design loadings in the notation of the U.S. Steel manual (9) are as follows:

LL moment: 838 ft-k midspan, 650 ft-k quarter

LL shear: 56.5 k support, 42.4 k quarter

Dead load 1: weight of element including main steel and deck concrete plus 1.1 lb per in. for transverse stiffeners

Dead load 2: 40 lb per sq ft of deck area for curbs and surfacing

Design shears at support and quarter points are obtained from the coefficients of Figure 2 for undeflecting support reactions. The proportions for the steel elements of Figure 8 at midspan and quarter are as follows:

Top flange: 12 by $^3/_4$ midspan, 12 by $^1/_2$ quarter

Web: 60.82 by $^3/_8$

Bottom flange: 40 by $^9/_{16}$ midspan, 40 by $^3/_8$ quarter

The total width of the bottom flange of a cell is 80 in.

Deflections at midspan are 2.17 in. for dead load 1, and 0.41 in. for dead load 2. The ratio of span to L + I deflection is 1,950 without consideration of the 10 percent excess live load. Transverse web stiffeners are spaced using $d = 11{,}000\ t/\sqrt{f_v}$. Stiffener spacing at the support is 54 in.; at the quarter a maximum spacing equal to the 60-in. vertical projection of the web is adequate. Plate stiffeners 6 by $^3/_8$ in. in cross section are used on the insides of the webs. Table 3 gives the allowable stress reserve available for warping stresses in the flanges when dead load and uniform flexural live load plus impact stresses (computed for an 84-in. effective flange width) are subtracted from the allowable stress.

Table 4 gives the properties for the BEF analogy as computed by the equations given in the Appendix for individual cells at midspan and quarter. For simplicity, the stiffener spacing is assumed to be uniform from support to quarter and quarter to midspan. The full 200-in. width of R/C deck associated with one cell of the two-cell bridge is considered to be effective in computing these properties. The values of I_c, Y_T, and Y_B are computed by using a depth of 65 in. from the center of deck to the center of bottom flange and by neglecting the moment of inertia of deck and flange about their own centroidal axes. The steel top flange is included in the transformed area of the deck slab.

An interior bracing system is designed to control distortion stresses. A limit of 4 ksi on the reversible distortion stress is applied. The worst torsional loading for distortion stress is a single truck at the outside of its lane (Fig. 2). For a wheel load P, the procedure of Figure 4 gives a torsional load of 1.12 P on the most severely loaded cell.

Cross braces at midspan and quarter points are tried. The dimensionless panel length of a midspan panel is given by $\beta\ell = 3.78 \times 10^{-3} (300) = 1.13$. The live load plus impact torsional load is obtained using an impact factor computed for the 25-ft panel length and a 16-kip wheel load, $P_{L+I} = 16(1.3) = 20.8$ kips, and the corresponding concentrated torsional load is P = 20.8 (1.12) = 23.3 kips.

To restrict σ_t to 4 ksi, the property σ_t/kW tabulated earlier is used to obtain a limit on kW = 4/271 = 0.0147 kips/in. Figure 9 shows the influence line for dimensionless deflection w at the middle of a midspan panel obtained by interpolation of the coefficients in Table 5 to $\beta\ell$ = 1.13. Note that by substitution from Eq. 2 in Eq. 3 the more convenient expression for dimensionless deflection, $w = (2k/\beta)\ W/P$, is obtained.

TABLE 3

FLANGE STRESSES
(in ksi)

Category	Top Flange		Bottom Flange	
	Midspan	Quarter	Midspan	Quarter
Dead load	18.08	17.13	12.56	13.09
HS20-44 L+I	1.71	1.31	5.90	6.04
Warping L+I	0.21	1.56	1.54	0.87

TABLE 4

SECTION PROPERTIES FOR BEF ANALOGY

Section Quantity	Unit of Measure	Equation (in Appendix)	Quarter	Midspan
Stiffener spacing	in.		54	60
Top width, a	in.		100	100
Bottom width, b	in.		80	80
Depth, h	in.		65	65
I_c	$in.^4$		1.49×10^5	1.88×10^5
Y_T	in.		13.35	15.75
Y_B	in.		51.65	49.25
v		9	1.68×10^{-2}	5.31×10^{-2}
k	$kips/in.^2$	8	1.08	1.12
β	$in.^{-1}$	2	3.98×10^{-3}	3.78×10^{-3}
Q/A_b	$kips/in.^3$	11	1.82×10^3	1.82×10^3
S_{web}	$in.^3/in.$	7	8.02×10^{-2}	7.22×10^{-2}
σ_t/kW	$in.^{-1}$	14	267	271

TABLE 5

INFLUENCE COEFFICIENTS FOR
DEFLECTION AT MIDDLE OF INTERIOR PANEL
[Values of $w = (8EI_b/P)\,\beta^3 W$]

Panel Length ($\beta\ell$)	Support Stiffness (q)	Distance of Unit Load From Midpanel (x/ℓ)				
		0.00	0.25	0.50	0.75	1.00
0.5	∞	0.011	0.007	0.000	-0.003	-0.004
	1,000	0.014	0.010	0.002	-0.002	-0.003
	100	0.036	0.031	0.021	0.012	0.006
	10	0.165	0.157	0.138	0.114	0.090
	1	0.574	0.562	0.530	0.486	0.433
1.0	∞	0.085	0.054	0.000	-0.027	-0.028
	100	0.099	0.067	0.012	-0.018	-0.023
	10	0.203	0.167	0.099	0.046	0.015
	1	0.604	0.558	0.455	0.342	0.235
2.0	∞	0.508	0.311	0.000	-0.134	-0.125
	10	0.549	0.355	0.044	-0.100	-0.106
	1	0.747	0.560	0.246	0.046	-0.034

The semilogarithmic plot is used to ease interpolation of values of q. For a 14-ft axle spacing, $x/\ell = 14/25 = 0.56$. A trial value of $q = 10$ is selected; the critical load position is centered about midpanel with the heavy axles, $w = 0.17 + 0.17 = 0.34$, as the front axle of P/4 makes a negligible contribution at $x/L = 0.84$. The derived value of kW is obtained from $kW = (p\beta/2)\,w = (23.3 \times 3.78 \times 10^{-3}/2) \times 0.34 = 0.0150$ kips/in., which is close to the limit derived above.

The area of brace required is obtained from the value of Q/A_b tabulated previously and from Eq. 5: $A_b = Q/(Q/A_b) = (qk\ell)/(Q/A_b) = 10 \times 1.12 \times 300/1820 = 1.85$ in.^{2}, which is provided by an angle $3\frac{1}{2}$ by $3\frac{1}{2}$ by $\frac{5}{16}$.

TABLE 6

INFLUENCE COEFFICIENTS FOR DEFLECTION AT MIDDLE OF END PANEL
[Values of $w = (8EI_b/P)\,\beta^3 W$]

Panel Length ($\beta\ell$)	Support Stiffness (q)	Distance of Unit Load From End (x/ℓ)				
		0.00	0.25	0.50	0.75	1.00
End Support Rigid, Interior Supports of Stiffness q						
0.5	∞	0.000	0.010	0.015	0.009	0.000
	1,000	0.000	0.012	0.017	0.012	0.003
	100	0.000	0.019	0.030	0.029	0.021
	10	0.000	0.041	0.072	0.086	0.087
	1	0.000	0.073	0.135	0.177	0.201
1.0	∞	0.000	0.081	0.113	0.068	0.000
	100	0.000	0.086	0.123	0.081	0.014
	10	0.000	0.121	0.189	0.168	0.106
	1	0.000	0.215	0.367	0.410	0.377
2.0	∞	0.000	0.445	0.632	0.372	0.000
	10	0.000	0.457	0.659	0.413	0.049
	1	0.000	0.514	0.782	0.604	0.273
End and Interior Supports of Stiffness q						
0.5	1,000	0.002	0.013	0.017	0.012	0.003
	100	0.018	0.032	0.038	0.033	0.023
	10	0.195	0.199	0.191	0.172	0.144
	1	1.253	1.145	1.032	0.909	0.781
1.0	100	0.008	0.091	0.126	0.082	0.014
	10	0.080	0.177	0.223	0.185	0.110
	1	0.648	0.692	0.690	0.605	0.475
2.0	10	0.022	0.469	0.664	0.414	0.049
	1	0.171	0.607	0.818	0.611	0.268

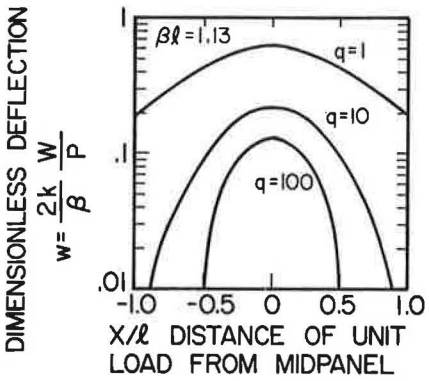

Figure 9. Influence line for midpanel deflection of analogous BEF.

TABLE 7

FREE END STIFFNESS OF CONTINUOUS BEF
[Values of $q^* = Q^*/k\ell$]

Panel Length ($\beta\ell$)	Interior Support Stiffness q			
	1	10	100	1,000
0.5	1.28	2.50	4.99	6.45
1.0	0.536	0.620	0.671	0.686
2.0	0.252	0.253	0.253	0.253

Similar computations for a panel between quarter and end of span give $\beta\ell = 3.98 \times 10^{-3} \times 300 = 1.20$ and also give kW limited to 4/267 = 0.0150 kips/in. The influence line for deflection at the middle of an end panel is interpolated from Table 6 by using values for equal end and interior support stiffnesses, and the results show cross-bracing angles $3\frac{1}{2}$ by $3\frac{1}{2}$ by $\frac{5}{16}$ to be adequate.

Bracing stresses are checked for the same loading—one truck at the outside of its lane. For the brace at midspan, influence coefficients are interpolated from Table 7 for $\beta\ell = 1.13$ and $q = A_b\,(Q/A_b)/k\ell = 2.09 \times 1{,}820/1.12 \times 300 = 11.3$. The derived value of R in Eq. 15 is 52.5 kips, and the brace force from $P_b = bL_bR/2h(a+b)$ becomes $80 \times 111 \times 52.5/2 \times 65 \times 180 = 19.9$ kips. The stress is $f_b = 19.9/2.09 = 9.5$ ksi. The use of an allowable stress, $F_b = 16{,}000 - 0.3\,(L/r)^2$ psi, indicates that the $3\frac{1}{2}$ by $3\frac{1}{2}$ by $\frac{5}{16}$ angles are adequate if connected at their point of intersection to restrain weak axis buckling.

The torsional loading of 1.12 P used in these computations is the most severe torsional loading for the individual cell. However, it acts with a flexural load from just one truck. The controlling flexure plus warping condition occurs for both lanes loaded. If the procedure given in Figure 4 and the axle load reactions in Figure 2 are used, the torsional load on the most severely twisted cell is 0.805 P for trucks left and 0.73 P for trucks center.

Warping stresses at midpanel of a midspan panel are computed for axle loads at that point using Eq. 4 to obtain M from m of Figure 12 and using $I_b = \frac{1}{4} I_c$ in computation of warping stresses caused by M:

$$\sigma_w = \frac{My}{I_b} = \frac{Pmy}{I_c\beta} = \frac{20.8 \times 0.805 \times 0.8 \times y}{1.88 \times 10^5 \times 3.78 \times 10^{-3}} = 0.0189\,y \qquad (1)$$

in which P is the 16-kip wheel load augmented by 30 percent impact, m = 0.8 is obtained from Figure 12 for $\beta\ell = 1.13$, and q = 11.3. For the top flange, y= 15.75 in., $\sigma_w = 0.30$ ksi, and the reserve for L + I warping stress is 0.21 ksi. For the bottom flange, y = 49.25 in., $\sigma_w = 0.93$ ksi, and the reserve for L + I warping stress is 1.54 ksi. The reserve is computed near midspan and the warping stress at the $\frac{3}{8}$ span point so that the design appears to be adequate. Adjacent axles are neglected in these computations because they would not be in the same panel and would tend to reduce warping stresses at the midpanel axle location.

The warping stresses at the middle of the end panel and midspan and quarter-braced points are checked in a similar manner using the influence coefficients given in the Appendix. These warping stresses are less severe than those evaluated earlier. The flange sections are adequate as selected initially.

SUMMARY AND CONCLUSIONS

An approximate analysis based on an analogy with the theory of beams on elastic foundations is developed for multicell box girders of deformable cross section. Procedures

are described for treating girders with longitudinally or transversely stiffened plate elements and with rigid or deformable interior diaphragms. Comparisons with results of refined analytical methods show that the BEF analogy predicts the magnitudes of warping and distortion stresses with an accuracy adequate for design when the objective in design is to keep these stresses small. Examples show that distortion stresses and, to a lesser extent, warping stresses may be significant in steel box girders of proportions appropriate for highway bridges. Design procedures should account for these stresses in a rational manner.

Refined analytical methods are available for evaluation of these stresses, but the complexity of the analyses tends to conceal the major design parameters. The BEF analogy lends itself to graphical presentation of the effects of design parameters on bridge response. In addition, the analogy contributes to the understanding of behavior as required for good design practice.

A direct design procedure using the BEF analogy is suggested for box-girder bridge design. The bridge cross section is proportioned by conventional means with consideration only of flexure and flexural shear stresses. After the properties of the cross section are defined, distortional effects are accounted for by selecting the diaphragm spacing and stiffness required to reduce distortion stresses to tolerable levels. Rather light, widely spaced diaphragms usually suffice. Box-girder bridges with interior diaphragms proportioned for limitation of distortion stresses provide an excellent distribution of flange stresses. For AASHO loadings, the peak live-load flange stress, including warping effects, generally appears to be less than 10 percent in excess of the average live-load flange stress at the section in question. This nearly uniform lateral distribution of stress gives box-girder bridges considerable economic potential.

ACKNOWLEDGMENTS

Much of the material presented here was prepared as part of an investigation sponsored by the American Iron and Steel Institute Committee of Steel Plate Producers and conducted in the Department of Civil Engineering at the University of Illinois, Urbana. The writer acknowledges substantial contributions made by S. R. Abdel-Samad and A. R. Robinson in the investigation, and many valuable suggestions from the following members of the AISI project Task Force: D. S. Wolford, W. E. Baumann, J. A. Gilligan, W. A. Milek, T. P. Noe, Jr., and I. M. Viest.

REFERENCES

1. Abdel-Samad, S. R., Wright, R. N., and Robinson, A. R. Analysis of Box Girders With Diaphragms. Jour. of the Struct. Div., Proc. ASCE, Vol. 94, No. ST10, Oct. 1968, pp. 2231-2255.
2. Scordelis, A. C. Analysis of Continuous Box Girder Bridges. College of Eng., Univ. of Calif., Berkeley, Rept. SESM-67-25, Nov. 1967.
3. Johnston, S. B., and Mattock, A. H. Lateral Distribution of Load in Composite Box Girder Bridges. Highway Research Record 167, 1967, pp. 25-33.
4. Goldberg, J. E., and Leve, H. L. Theory of Prismatic Folded Plate Structures. International Assn. for Bridge and Structural Eng., Zurich, Vol. 17, 1957.
5. Wright, R. N., Abdel-Samad, S. R., and Robinson, A. R. BEF Analogy for Analysis of Box Girders. Jour. of the Struct. Div., Proc. ASCE, Vol. 94, No. ST7, July 1968, pp. 1719-1743.
6. Abdel-Samad, S. R. Analysis of Multicell Box Girders With Diaphragms. Univ. of Illinois, Urbana, PhD dissertation, 1967.
7. Standard Specifications for Highway Bridges. The American Association of State Highway Officials, Washington, 1965.
8. Design Manual for Orthotropic Steel Plate Deck Bridges. American Institute of Steel Construction, New York, 1963.
9. Highway Structures Design Handbook. United States Steel Corp., 1965.
10. Hetenyi, M. Beams and Plates on Elastic Foundations and Related Problems. Applied Mechanics Reviews, Vol. 19, No. 2, Feb. 1966, p. 95.

Appendix

SUMMARY OF THE BEF ANALOGY

The equations and influence coefficients required to use the beam on elastic foundation analogy in the design of box girders are presented here without derivations, which are available elsewhere (5, 11). The analogy is illustrated in Figure 10. The analogous BEF has a foundation modulus k, proportional to the resistance of the box cell to deformation of its cross section; a flexural stiffness EI_b, proportional to the warping stiffness of the box cell; and a support stiffness Q, proportional to the stiffness of a diaphragm or cross bracing of the box cell. Span length or panel length between intermediate supports for the analogous BEF is the same as the span length or panel length between diaphragms of the box cell. The loading on the analogous BEF is the same in magnitude and longitudinal distribution as the component of the torsional load acting on one side of the box cell. The resulting deflection of the BEF is proportional to the transverse flexural stresses in the plates of the box cell. The resulting moment in the beam on elastic foundation is proportional to the longitudinal warping stresses in the box cell. These stresses arise in the box cell because the type of torsional load shown in Figure 10 distorts the cross section as well as twists it. The shearing and longitudinal warping stresses from the pure torsional effect are rarely significant and are not considered here.

Behavior of Beams on Elastic Foundation

Extensive literature is available on the analysis of beams on elastic foundations, as described by Hetenyi (10), so the presentation here is limited to the definition of terms used in development of influence coefficients for design. A parameter

$$\beta = 4\sqrt{\frac{k}{4EI_b}} \qquad (2)$$

relates the foundation modulus and flexural stiffness of the BEF in a manner leading to convenient dimensionless representation of behavior. The deflection W of a BEF

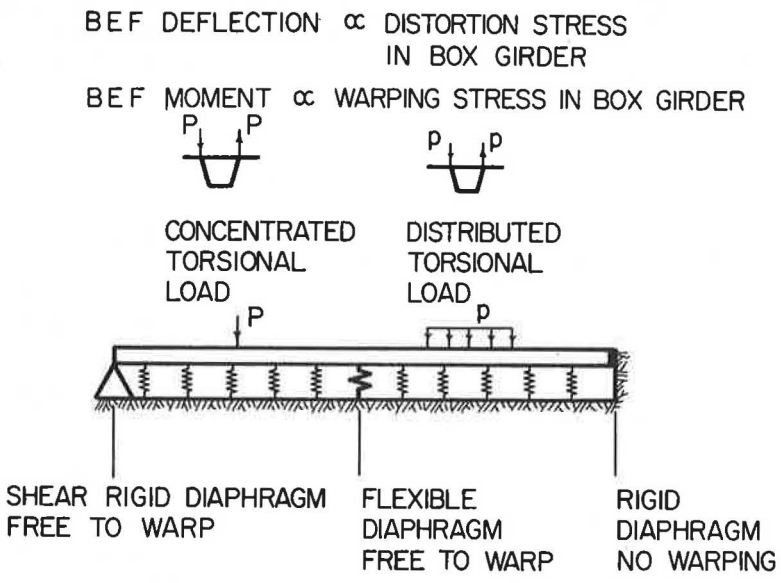

Figure 10. Analogy between box girder and BEF.

under concentrated load P is expressed nondimensionally as

$$w = \frac{8EI_b\beta^3}{P} W \tag{3}$$

and the bending moment M is expressed nondimensionally by

$$m = \frac{4\beta}{P} M \tag{4}$$

These expressions are convenient because as the BEF becomes long, maximum values of both w and m approach 1. The stiffness Q of a support is expressed nondimensionally as

$$q = \frac{Q}{k\ell} \tag{5}$$

where ℓ is the panel length between supports.

The behavior of a BEF that is continuous over many regularly spaced interior supports is illustrated in Figures 11, 12, and 13. Figure 11 shows that the deflection under a concentrated load at the middle of a panel is proportional to the distortion stress in a box cell at a midpanel location of a concentrated torsional load. The reduction of panel length by closer spacing of supports produces rapid decrease in the deflection (or distortion stress) for dimensionless panel lengths $\beta\ell < 2$. The effect of support stiffness q is illustrated, and it should be noted that a support of given actual stiffness Q increases in dimensionless stiffness q as ℓ is reduced. Figure 12 shows that the moment under a concentrated load at the middle of a panel is proportional to the warping stress in a box cell at a midpanel location of a concentrated torsional load. It is evident that moment is not reduced as sharply as is deflection by reduction of panel length or increase of support stiffness. Figure 13

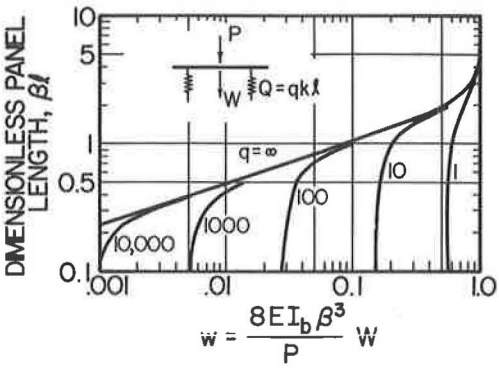

Figure 11. Midpanel deflection of continuous BEF (analogous to distortion stress).

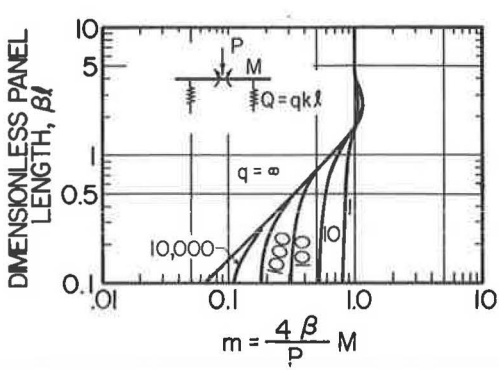

Figure 12. Midpanel moment of continuous BEF (analogous to warping stress).

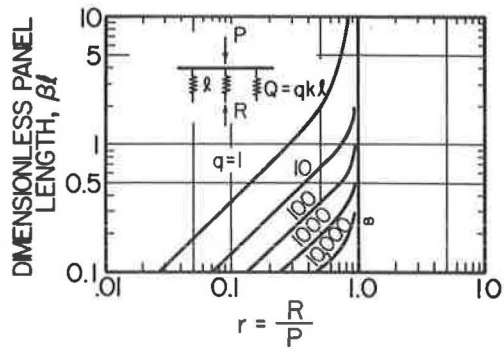

Figure 13. Interior support reaction of continuous BEF (analogous to diaphragm stress).

TABLE 8

INFLUENCE COEFFICIENTS FOR MOMENT AT MIDDLE OF INTERIOR PANEL
[Values of m = (4β/P) M]

Panel Length ($\beta\ell$)	Support Stiffness (q)	Distance of Unit Load From Midpanel (x/ℓ)				
		0.00	0.25	0.50	0.75	1.00
0.5	∞	0.341	0.131	0.000	-0.056	-0.058
	1,000	0.350	0.139	0.006	-0.052	-0.058
	100	0.406	0.191	0.046	-0.033	-0.061
	10	0.598	0.374	0.200	0.076	-0.006
	1	0.861	0.629	0.433	0.271	0.141
1.0	∞	0.671	0.254	0.000	-0.107	-0.110
	100	0.679	0.262	0.007	-0.102	-0.108
	10	0.744	0.321	0.049	-0.086	-0.122
	1	0.905	0.472	0.170	-0.018	-0.116
2.0	∞	1.099	0.347	0.000	-0.113	-0.105
	10	1.090	0.337	-0.009	-0.119	-0.108
	1	1.052	0.296	-0.053	-0.157	-0.140

shows that the reaction at an interior support for a concentrated load at the support is proportional to the stresses in a diaphragm or cross bracing of a box cell at the location of a concentrated torsional load.

Influence coefficients are given in Tables 5 through 13 for BEF response quantities of interest in box girder design. A range of dimensionless panel lengths $0.5 \leq \beta\ell \leq 2$ is considered. This is the range of practical importance. For shorter panel lengths the elastic foundation effect is small; the behavior of the box cell may be represented by a beam of flexural rigidity EI_b on flexible supports of stiffness Q. For greater panel lengths the effect of the interior supports is small, and the box cell may be represented as an infinitely long BEF. Distortion stresses in a box cell are most critical at midpanel where the restraining effect of diaphragms on cross section deformation is

TABLE 9

INFLUENCE COEFFICIENTS FOR MOMENT AT MIDDLE OF END PANEL
[Values of m = (4β/P) M]

Panel Length ($\beta\ell$)	Support Stiffness (q)	Distance of Unit Load From End (x/ℓ)				
		0.00	0.25	0.50	0.75	1.00
End Support Rigid, Interior Supports of Stiffness q						
0.5	∞	0.000	0.187	0.399	0.161	0.000
	1,000	0.000	0.193	0.410	0.176	0.014
	100	0.000	0.227	0.472	0.255	0.093
	10	0.000	0.302	0.612	0.440	0.293
	1	0.000	0.357	0.718	0.587	0.467
1.0	∞	0.000	0.361	0.781	0.312	0.000
	100	0.000	0.367	0.792	0.328	0.016
	10	0.000	0.409	0.870	0.426	0.112
	1	0.000	0.496	1.031	0.637	0.333
2.0	∞	0.000	0.459	1.204	0.398	0.000
	10	0.000	0.458	1.201	0.394	-0.004
	1	0.000	0.454	1.192	0.378	-0.026
End and Interior Supports of Stiffness q						
0.5	1,000	-0.006	0.188	0.407	0.175	0.014
	100	-0.046	0.194	0.451	0.243	0.088
	10	-0.183	0.155	0.500	0.360	0.240
	1	-0.463	-0.040	0.387	0.317	0.253
1.0	100	-0.009	0.361	0.789	0.326	0.016
	10	-0.080	0.354	0.836	0.410	0.108
	1	-0.429	0.180	0.817	0.508	0.268
2.0	10	-0.031	0.441	1.194	0.392	-0.004
	1	-0.249	0.320	1.139	0.368	-0.019

TABLE 10

INFLUENCE COEFFICIENTS FOR MOMENT AT INTERIOR SUPPORT
[Values of m = (4β/P) M]

Panel Length ($\beta\ell$)	Support Stiffness (q)	Distance of Unit Load From Interior Support (x/ℓ)				
		0.00	0.25	0.50	0.75	1.00
0.5	∞	0.000	-0.153	-0.158	-0.084	-0.000
	1,000	0.033	-0.126	-0.146	-0.090	-0.022
	100	0.182	-0.003	-0.083	-0.094	-0.070
	10	0.492	0.276	0.119	0.011	-0.057
	1	0.813	0.582	0.388	0.230	0.103
1.0	∞	0.000	-0.304	-0.312	-0.166	0.000
	100	0.046	-0.265	-0.289	-0.167	-0.031
	10	0.279	-0.077	-0.203	-0.187	-0.112
	1	0.745	0.330	0.064	-0.086	-0.153
2.0	∞	0.000	-0.552	-0.515	-0.250	0.000
	10	0.095	-0.473	-0.468	-0.240	-0.030
	1	0.508	-0.151	-0.316	-0.239	-0.103

smallest. Influence coefficients for BEF deflection at midpanel are given in Table 5 for an interior panel and in Table 6 for an end panel. The end panel may be critical if end diaphragms are not substantially stiffer than interior diaphragms. Coefficients are given in Table 6 for rigid end supports and for end supports of the same stiffness as the interior supports. Interpolation for finite end support stiffness q_e is given by

$$f = f_r + \frac{q^* + q}{q^* + q_e} (f_q - f_r) \qquad (6)$$

where f is the interpolated coefficient, f_r is the coefficient for rigid end support with interior supports of stiffness q, f_q is the coefficient for all supports of stiffness q, and q^* is the end stiffness of the BEF for no support at the end. Values of q^* are given in Table 7.

TABLE 11

INFLUENCE COEFFICIENTS FOR MOMENT AT FIRST INTERIOR SUPPORT
[Values of m = (4β/P) M]

Panel Length ($\beta\ell$)	Support Stiffness (q)	Distance of Unit Load From End (x/ℓ)				
		0.00	0.25	0.50	0.75	1.00
End Support Rigid, Interior Supports of Stiffness q						
0.5	∞	0.000	-0.125	-0.201	-0.176	0.000
	1,000	0.000	-0.113	-0.179	-0.148	0.028
	100	0.000	-0.044	-0.052	0.013	0.188
	10	0.000	0.108	0.232	0.390	0.596
	1	0.000	0.223	0.453	0.696	0.959
1.0	∞	0.000	-0.245	-0.394	-0.347	0.000
	100	0.000	-0.230	-0.366	-0.311	0.039
	10	0.000	-0.129	-0.180	-0.073	0.274
	1	0.000	0.089	0.228	0.466	0.847
2.0	∞	0.000	-0.351	-0.609	-0.598	0.000
	10	0.000	-0.329	-0.561	-0.522	0.091
	1	0.000	-0.221	-0.332	-0.170	0.496
End and Interior Supports of Stiffness q						
0.5	1,000	-0.012	-0.122	-0.184	-0.150	0.028
	100	-0.089	-0.109	-0.094	-0.010	0.179
	10	-0.341	-0.165	0.024	0.240	0.497
	1	-0.769	-0.435	-0.097	0.248	0.603
1.0	100	-0.015	-0.240	-0.372	-0.313	0.039
	10	-0.117	-0.210	-0.230	-0.097	0.268
	1	-0.525	-0.298	-0.033	0.308	0.768
2.0	10	-0.007	-0.332	-0.563	-0.523	0.031
	1	-0.077	-0.263	-0.348	-0.174	0.499

TABLE 12

INFLUENCE COEFFICIENTS FOR REACTION AT INTERIOR SUPPORT
[Values of r = R/P]

Panel Length ($\beta\ell$)	Support Stiffness (q)	Distance of Unit Load From Interior Support (x/ℓ)				
		0.00	0.25	0.50	0.75	1.00
0.5	∞	1.000	0.881	0.600	0.269	0.000
	1,000	0.944	0.834	0.576	0.279	0.050
	100	0.725	0.663	0.512	0.324	0.153
	10	0.382	0.365	0.321	0.262	0.199
	1	0.139	0.136	0.128	0.117	0.104
1.0	∞	1.000	0.876	0.591	0.263	0.000
	100	0.955	0.835	0.562	0.259	0.035
	10	0.736	0.662	0.490	0.287	0.112
	1	0.288	0.268	0.221	0.164	0.108
2.0	∞	1.000	0.815	0.479	0.184	0.000
	10	0.907	0.737	0.430	0.164	0.012
	1	0.498	0.408	0.246	0.106	0.020

Warping stresses in a box cell may be critical either near midpanel or at a diaphragm. Tables 8 and 9 give influence coefficients for midpanel moment in a BEF for interior and end panels respectively. Tables 10 and 11 give influence coefficients for moment in a BEF at interior and first interior supports respectively. Equation 6 remains applicable to Tables 9 and 11 for determining the effect of a different finite end support stiffness.

Stresses in the diaphragms or bracing of a box cell are proportional to the support reaction of the analogous BEF. Tables 12 and 13 give influence coefficients for interior and end support reactions respectively. Equation 6 may be used to interpolate for different, finite end support stiffness in Table 13.

TABLE 13

INFLUENCE COEFFICIENTS FOR REACTION AT END SUPPORT
[Values of r = R/P]

Panel Length ($\beta\ell$)	Support Stiffness (q)	Distance of Unit Load From End (x/ℓ)				
		0.00	0.25	0.50	0.75	1.00
End Support Rigid, Interior Supports of Stiffness q						
0.5	∞	1.000	0.686	0.399	0.161	0.000
	1,000	1.000	0.692	0.409	0.175	0.014
	100	1.000	0.726	0.472	0.254	0.092
	10	1.000	0.800	0.610	0.438	0.291
	1	1.000	0.855	0.715	0.583	0.463
1.0	∞	1.000	0.675	0.384	0.153	0.000
	100	1.000	0.678	0.389	0.160	0.007
	10	1.000	0.697	0.425	0.205	0.051
	1	1.000	0.736	0.498	0.300	0.150
2.0	∞	1.000	0.546	0.228	0.062	0.000
	10	1.000	0.545	0.226	0.058	-0.005
	1	1.000	0.539	0.214	0.040	-0.028
End and Interior Supports of Stiffness q						
0.5	1,000	0.994	0.688	0.407	0.174	0.014
	100	0.952	0.692	0.449	0.242	0.088
	10	0.800	0.641	0.488	0.350	0.233
	1	0.438	0.375	0.313	0.256	0.203
1.0	100	0.993	0.673	0.387	0.159	0.007
	10	0.942	0.656	0.400	0.193	0.048
	1	0.651	0.479	0.324	0.195	0.098
2.0	10	0.975	0.531	0.220	0.057	-0.005
	1	0.799	0.431	0.171	0.032	-0.022

Relationships Between Box Cell and BEF Properties

The expressions given apply to a single-cell symmetrical box cell as shown in cross section in Figure 14. The cell may be of composite construction if the properties appearing in the expressions are transformed to a reference Young's modulus E. Some or all of the plates of the box cell may be stiffened so that distinct plate properties are defined: t denotes the average thickness effective in longitudinal extension, which includes the area per unit width of regularly spaced longitudinal stiffeners; D denotes the plate flexural stiffness in transverse bending. For an unstiffened plate, $D = Et^3/12\ (1 - \upsilon^2)$ in which υ is Poisson's ratio. For transversely stiffened plates, D is the average flexural stiffness of a plate strip of unit dimension in the direction of the span of the box cell. This property may be evaluated by procedures given in the AISC Design Manual for Orthotropic Bridges (8). Each transverse stiffener acts in flexure with an effective width of plate d* such that

$$d^* = \frac{d_s \tanh\left(5.6\,\frac{d_s}{a}\right)}{\left(5.6\,\frac{d_s}{a}\right)(1 - \upsilon^2)} \tag{7}$$

in which d_s is the spacing of the transverse stiffeners and a is the span of the plate in the cross section of the box cell (dimension a, b, or c of Fig. 14). D is evaluated by computing the moment of inertia I_s of the transverse stiffener cross section acting with a plate flange of width d*, so that $D = EI_s/d_s$. Transverse flexural stresses are computed using a section modulus per unit width, $S = I_s/cd_s$, where c is the distance to the extreme fiber for the combined section of stiffener and effective plate flange.

The property of the box cell corresponding to the foundation modulus k of the analogous BEF is

$$k = \frac{24\,(a + b)}{ab\left\{\frac{c}{D_c}\left[\frac{2ab}{a + b} - \nu(2\,a + b)\right] + \frac{a^2}{D_a}\left[\frac{b}{a + b} - \nu\right]\right\}} \tag{8}$$

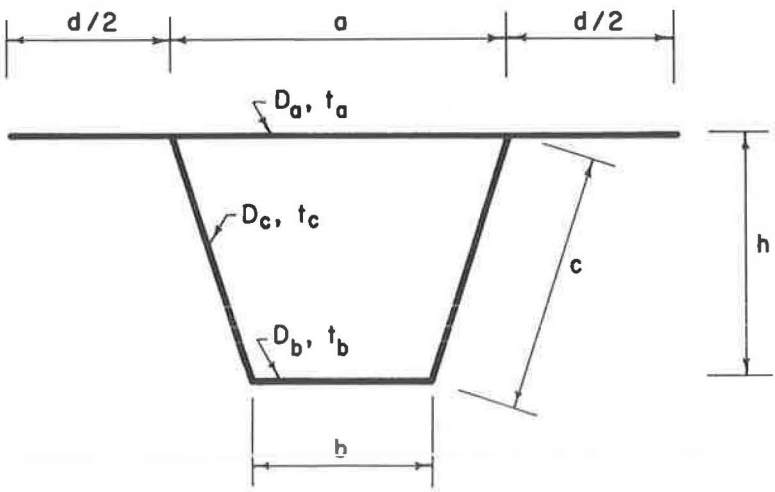

Figure 14. Notation for proportions of box girder cell.

in which a, b, and c are the dimensions shown in Figure 14, the D's are the corresponding transverse flexural rigidities of the plates, and v is given as follows:

$$v = \frac{\frac{1}{D_c}\left[(2a + b)\,abc\right] + \frac{1}{D_a}(ba^3)}{(a + b)\left[\frac{a^3}{D_a} + \frac{2c\,(a^2 + ab + b^2)}{D_c} + \frac{b^3}{D_b}\right]} \tag{9}$$

The property of the box cell corresponding to the moment of inertia I_b of the analogous BEF is given approximately by

$$I_b \sim \frac{I_c}{4} \tag{10}$$

in which I_c is the moment of inertia of the box cell cross section shown in Figure 14 about its horizontal centroidal axis. The exact expression for I_b is developed elsewhere (5); it is shown there that the approximation leads to nearly correct, generally conservative values of warping and distortion stresses.

The property of the box cell corresponding to the stiffness of supports of the analogous BEF is the resistance of cross bracing or diaphragms to distortion of the box cross section. For a pair of cross braces, each of area A_b, Young's modulus E_b, and length L_b (connecting the top of one web to the bottom of the other),

$$Q = E_b A_b \frac{4h^2\left(1 + \frac{a}{b}\right)^2}{L_b^3} \tag{11}$$

in which a, b, and h are dimensions shown in Figure 14. The stiffness of a plate diaphragm of shear modulus G_p and thickness t_p is approximated by considering an equivalent pair of cross braces that leads to the following expression:

$$Q = \frac{4G_p t_p\,(a + b)\,h}{b^2} \tag{12}$$

After analysis of the analogous BEF, transverse flexural stresses in the plates of the box cell are obtained from the deflection W of the BEF. Maximum stresses occur at intersections of web and flange plates; the stress at the bottom is given by

$$\sigma_t = \frac{bv}{2S}\,kW \tag{13}$$

and at the top by

$$\sigma_t = \frac{a}{2S}\left(\frac{b}{a + b} - v\right) kW \tag{14}$$

where S is the section modulus of the web or flange plate, v is given by Eq. 9, and a and b are the dimensions shown in Figure 14.

Warping stresses are computed in a manner consistent with the approximate I_b of Eq. 10. They are related to the moment M of the analogous BEF by the flexure formula, $f = My/I_b$, in which y is the distance from the flexural centroidal axis corresponding to I_c. Note that $I_b = I_c/4$ is used as the moment of inertia.

Stresses in cross bracing or diaphragms are computed from the reaction R of the analogous BEF. For a pair of cross braces, the force in each is

$$P_b = \frac{bL_b}{2h\,(a + b)}\,R \tag{15}$$

The shear stress in a plate diaphragm is approximately

$$f_v = \frac{a\,R}{h\,(a + b)\,t_p} \tag{16}$$

Reference

11. Dabrowski, R. Der Schubverformungseinfluss auf die Wölbkrafttorsion der Kastenträger mit verformbarem biegesteifem Profil. Der Bauingenieur, 40 1965, Heft 11, pp. 444-449.